Journal of Applied Biomedicine 16 (2018) 66–74

Contents lists available at ScienceDirect

Journal of Applied Biomedicine

journal homepage: www.elsevier.com/locate/jab

Original research article

DNA repair inhibitors as radiosensitizers in human lung cells

Kamila Ďurišová[a], Lucie Čecháková[a], Petr Jošt[b,c], Zuzana Šinkorová[a], Adéla Kmochová[a], Jaroslav Pejchal[a,b], Martin Ondrej[a], Jiřina Vávrová[a], Aleš Tichý[a,c,*]

[a] University of Defence in Brno, Faculty of Military Health Sciences in Hradec Králové, Department of Radiobiology, Hradec Králové, Czech Republic
[b] University of Defence in Brno, Faculty of Military Health Sciences in Hradec Králové, Department of Toxicology and Military Pharmacy, Hradec Králové, Czech Republic
[c] University Hospital Hradec Králové, Biomedical Research Centre, Hradec Králové, Czech Republic

ARTICLE INFO

Article history:
Received 12 December 2016
Received in revised form 23 May 2017
Accepted 24 October 2017
Available online 27 November 2017

Keywords:
DNA repair
DNA-PK
ATM
ATR
Inhibition
Ionizing radiation
Lung cancer

ABSTRACT

The aim of this study was to compare the effects of DNA repair inhibitors in the context of radiosensitization of human lung cells. The radio-sensitizing effects of NU7441 (1 mM), an inhibitor of DNA-dependent protein kinase (DNA-PK); KU55933 (10 μM), an inhibitor of ataxia-telangiectasia mutated kinase (ATM); and VE-821 (10 μM), an inhibitor of ATM-related kinase (ATR) were tested by the xCELLigence system for monitoring proliferation, fluorescence microscopy for DNA damage detection, flow-cytometry for cell cycle and apoptosis analysis and western blotting and ELISA for determination of DNA repair proteins. We employed normal human lung fibroblasts (NHLF, p53-wild-type) and non-small cell lung cancer cells (H1299, p53-negative). DNA-PK inhibition (by NU7441) in combination with ionizing radiation (IR) increased the number of double strand breaks (DSB), which persisted 72 h after irradiation in both cell lines. Additionally, NU7441 and KU55933 in combination with IR caused G2-arrest. ATR inhibitor (VE-821) together with IR markedly inhibited proliferation and induced G2/M arrest accompanied by apoptosis in H1299, but not in NHLF cells, and thus diminished DNA-repair of tumour cells but not normal lung fibroblasts. Our findings indicate that ATR inhibition could be a promising therapeutic strategy in p53-deficient lung tumours.
© 2017 Faculty of Health and Social Sciences, University of South Bohemia in Ceske Budejovice. Published by Elsevier Sp. z o.o. All rights reserved.

Introduction

Lung cancer is one of the most commonly diagnosed cancers and it is responsible for approximately one third of all cancer-related deaths. Non-small cell lung cancer (NSCLC) represents around 81% of all cases of lung cancer and it is often fatal (Gérard and Debruyne, 2009; Schiller et al., 2002). Although ionizing radiation (IR) is crucial for treatment of inoperable cases (Christodoulou et al., 2014), the DNA damage caused by radiotherapy is often insufficient. Specifically, IR treatment of cancer induces the DNA damage response (DDR), leading to effective repair of the damage and survival of the cancer cells. Hence there is an increasing interest in small-molecule inhibitors capable of decreasing activation of pivotal DNA repair kinases and leading to subsequent radio-sensitization of cancer cells.

An attractive approach to enhancing radio-sensitivity could be by targeting phosphatidylinositol-3-kinase-related kinases (PIKK): ataxia-telangiectasia mutated kinase (ATM), DNA-dependent protein kinase (DNA-PK), and ATM-related kinase (ATR) (Andrs et al., 2015). Since these kinases are key players in DDR and DNA repair pathways, they could significantly enhance the tumour-killing effects of existing irradiation and/or chemotherapeutics.

ATM plays a crucial role in DNA repair and cell cycle regulation via p53 phosphorylation and its stabilization directly or indirectly by phosphorylation of CHK2 (Chaturvedi et al., 1999; Hirao et al., 2000). Protein p53 also known as the “genome guardian” is responsible for cell fate by directing the cell towards either cell-cycle arrest and survival or cell death (Lane, 1992). DNA-PK is a pivotal component of the non-homologous end-joining repair pathway of double strand breaks (DSB) (Baumann and West, 1998). ATR regulates single-stranded DNA repair which occurs either during normal replication or abnormal replication caused by DNA-

* Author for correspondence: University of Defence in Brno, Faculty of Military Health Sciences in Hradec Králové, Department of Radiobiology, Trebesska 1575, 500 01 Hradec Králové, Czech Republic.
E-mail address: ales.tichy@unob.cz (A. Tichý).

https://doi.org/10.1016/j.jab.2017.10.008
1214-021X/© 2017 Faculty of Health and Social Sciences, University of South Bohemia in Ceske Budejovice. Published by Elsevier Sp. z o.o. All rights reserved.

damaging agents such as IR (Hurley et al., 2007; Toledo et al., 2013). ATR prevents cells from entering into S-phase or progression through S-phase indirectly via CHK1 phosphorylation (Zhao et al., 2002).

Previously we assessed the radio-sensitizing effect of DNA-PK inhibitor NU7441 on the model cell line of T-lymphocyte leukemia (MOLT-4) leading to an increased level of DSB and subsequent activation of apoptosis (Tichy et al., 2014). We also compared the effects of the ATM inhibitor KU55933 and the ATR inhibitor VE-821 in promyelocytic leukemia cells (HL-60), concluding that ATR inhibition induced more pronounced radio-sensitization and abrogated G2 cell cycle arrest compared to ATM inhibition (Vávrová et al., 2013).

In this study, we have compared the response to IR in combination with three different DNA repair kinase inhibitors in p53-proficient normal human lung fibroblasts (NHLF) and p53-deficient non-small cell lung cancer cells (H1299), which are relevant to radiotherapy. We employed NU7441, a specific inhibitor of DNA-PK; KU55933, a specific inhibitor of ATM; and VE-821, a specific inhibitor of ATR. The aim of this study was to compare the effects on DDR of the inhibitors alone and in combination with IR, to assess the formation of DSB and progression of the cell cycle or cell death, and to evaluate their potential for radio-sensitization.

Materials and methods

Cell cultures and culture conditions

NHLF cells (normal human lung fibroblasts) cells were obtained from the Lonza Group Ltd (Basel, Switzerland). The cells were cultured in a humidified atmosphere with 5% CO_2 at 37 °C in Dulbecco's modified Eagle medium (DMEM) with high glucose and GlutaMAX™ supplement (Life Technologies, NY, USA), and further supplemented with 10% fetal bovine serum (Gibco, Paisley, UK), 150 UI/ml penicillin and 50 μg/ml streptomycin (Sigma-Aldrich, St. Louis, MO, USA). H1299 cells (non-small cell lung cancer cells) were obtained from the American Type Culture Collections (Manassas, VA, USA). The cells were cultured in a humidified atmosphere with 5% CO_2 at 37 °C in RPMI medium 1640 (Gibco, Paisley, UK) supplemented with 10% fetal bovine serum, 150 UI/ml penicillin and 50 μg/ml streptomycin.

The cultures were split twice a week by dilution to a concentration of 5×10^4 cells/ml. The cell counts were conducted with a hemocytometer by assaying the cell membrane integrity with trypan blue exclusion. The cell batch obtained from the company was cultivated in order to obtain aliquots with a sufficient number of cells. After that, aliquots were frozen and hence the cells used in this work all came from the same batch. A cell line with up to 12 passages was used for this study.

Gamma irradiation

The cells were irradiated at room temperature using a ^{60}Co gamma-ray source with a dose-rate of 0.5 Gy.min^{-1}, at a distance of 1 m from the source. After irradiation the flasks were placed in a 37 °C incubator with 5% CO_2 and the cells were removed at various intervals after irradiation for analysis.

Inhibitor treatment

We employed the most specific inhibitors to date. We added inhibitors to the final concentration 1 μM NU7441 (Tocris Bioscience, Bristol, UK), 10 μM KU55933 (Merck Milipore Billerica, MA, USA) and 1 μM VE-821 (APIs Chemical Co., Ltd, Shanghai, China) respectively, dissolved in dimethyl sulfoxide (DMSO) (Sigma-Aldrich, St. Louis, MO, USA) to the cells 30 min prior to irradiation. The concentration and the incubation time were based on our previous experiments and other papers (Ciszewski et al., 2014; Ćmielová et al., 2015; Kmochova et al., 2016; Vávrová et al., 2013).

Real-time cell viability analysis

The xCELLigence label-free system is based on impedance readout to quantify cellular status in real-time. The xCELLigence system was used according to the manufacturer's instructions (ACEA Biosciences, Inc.; San Diego, CA, USA). Briefly, after measuring the background reading, a suitable number of cells are seeded on to the 96-well plate integrated with gold microelectrode arrays. After application of low voltage, an electric field between the electrodes is created, which interacts with the ionic environment of the growth medium inside the wells and is modulated by the number of cells covering the electrodes, the morphology, and the strength of cell attachment. The changes in impedance are continuously measured and spatially integrated, and expressed over time by the instrument software as the cell index (CI). The real-time monitoring of cell viability enables distinction between different kind of anomalies of cell viability, such as senescence, cell toxicity, cell death and cell cycle arrest (represented as reduced proliferation). Moreover, the xCELLigence can be used to identify the best time interval for measuring changes, for example cellular or biochemical changes, in end-point assays, such as the right time point for apoptosis measurement; or mRNA or protein expression changes in siRNA studies. Last but not least, it can also be used for assessment of cell barrier function and cell differentiation, and in hypoxia studies (more applications can be found on the manufacturer's website www.aceabio.com). The higher the measured CI the higher is the number of the cells covering the electrodes. The cells (8×10^3/well for NHLF and 10^3/well for H1299) were allowed to sediment and attach at room temperature (RT), and then placed on the xCELLigence analyser unit in the 37 °C incubator with 5% CO_2. The data were collected every hour for 10 days. The presented CI values were counted from 6 replicate values.

Epifluorescence microscopy

The cells were seeded on underlying glasses at different time intervals after irradiation (1, 24, and 72 h). The underlying glasses were gently washed twice for 2 min each in PBS (Sigma-Aldrich, St. Louis, MO, USA) at 37 °C, fixed with 4% paraformaldehyde (Sigma-Aldrich, St. Louis, MO, USA) in PBS for 15 min at RT, rinsed quickly twice in PBS, then washed in PBS for 5 min, permeabilized in 0.2% Triton X-100/PBS (Sigma-Aldrich, St. Louis, MO, USA) for 17 min at RT, rinsed quickly twice in PBS and then washed in PBS for 5 min. Before incubation with the primary antibody (overnight at 4 °C), the cells were blocked with 7% inactivated FBS + 2% bovine serum albumin/PBS for 30 min at RT. The rabbit antibody against H2AX phosphorylated at serine 139 (γH2AX) was from Merck Millipore (Billerica, MA, USA). The secondary antibody was affinity-purified donkey anti-rabbit-FITC-conjugated or anti-rabbit-Cy3-conjugated obtained from Jackson Laboratory (West Grove, PA, USA). The secondary antibody was applied to each slide – after their pre-incubation with 5.5% of donkey serum/PBS (Sigma-Aldrich, St. Louis, MO, USA) for 30 min at RT – and incubated for 1 h in the dark at RT. This was followed by washing (quickly twice, then for 5 min) in PBS. After brief washing in deionized water, the DNA of the cells was counterstained with 1 μM DAPI (Cell Signalling Technology, Inc., MA, USA), and Vectashield medium (Vector Laboratories, Burlingame, CA) was used for the final mounting of the samples.

A Nikon Eclipse Ti epifluorescence microscope (Nikon Corporation, Amsterdam, NLD) equipped with Nikon Plan Apo VC 60x/1.40 oil immersion objective was used for examining nuclear foci (magnification 600). Fluorescence was evaluated in 50 cells per group and γH2AX foci were determined by ImagePro 5.1 software (Media Cybernetics, Bethesda, MD, USA).

Enzyme-linked immunosorbent assay

We used PathScan Phospho – CHK1 (S317) and CHK2 (T68) Sandwich ELISA Kits (Cell Signalling Technology, Inc., MA, USA) according to the protocol of the manufacturer. After incubation of the cell lysates with the primary and the HRP-linked secondary antibody, a substrate and then a stop solution were added and a positive reaction was quantified by spectrophotometric determination at 450 nm on SpectraMax PARADIGM™ Microplate Detection Platform (Beckman Coulter, Brea, CA, USA).

Flow cytometric analysis

Flow cytometry data were acquired and analysed on the CyAn ADP™ flow cytometric analyser (Beckman Coulter, Prague, CZE) using Summit 4.3 acquisition/analysis software. For cell cycle analysis the untreated control and irradiated cells were collected, washed with cold PBS and fixed with 70% ethanol. Afterwards, the cells were stained with propidium iodide (PI) in Vindelov's solution at RT in the dark for 10 min. Three independent experiments were performed.

Apoptosis was monitored by Annexin V-FITC (Dako, Glostrup, DEN) due to its specific binding to superficially exposed phosphatidylserine occurring in the cells upon programmed cell death initiation. The necrotic cells were visualized according to PI incorporation into DNA through the disrupted cell membranes. Three independent experiments were performed.

Electrophoresis and western blotting

At various time intervals after irradiation, the cells were washed with PBS and lysed. The whole-cell extracts were prepared by lysis in 500 μl of lysis buffer (137 mM NaCl; 10% glycerol; 1% *n*-octyl-β-glucopyranoside; 50 mM NaF; 20 mM Tris, pH = 8; 1 mM Na_3VO_4; 1 tablet of protein inhibitors Complete™ Mini, Roche, Basel, CHN). The lysates containing equal amounts of protein (30 μg) were loaded onto a 12% SDS polyacrylamide gel. After electrophoresis, the proteins were transferred to a polyvinylidene difluoride membrane (BioRad, Hercules, CA, USA) and hybridized with an appropriate antibody: anti-CHK2, anti-CHK1, anti-CHK2 T68, anti-CHK1 S296, anti-CHK1 S329, anti-LC3I/II (all from Cell Signalling Technology, Inc., MA, USA) and anti-β-actin (Sigma-Aldrich, St. Louis, MO, USA). After washing, the blots were incubated with the secondary peroxidase-conjugated antibody (Dako, Glostrup, DEN) and the signal was developed with the ECL

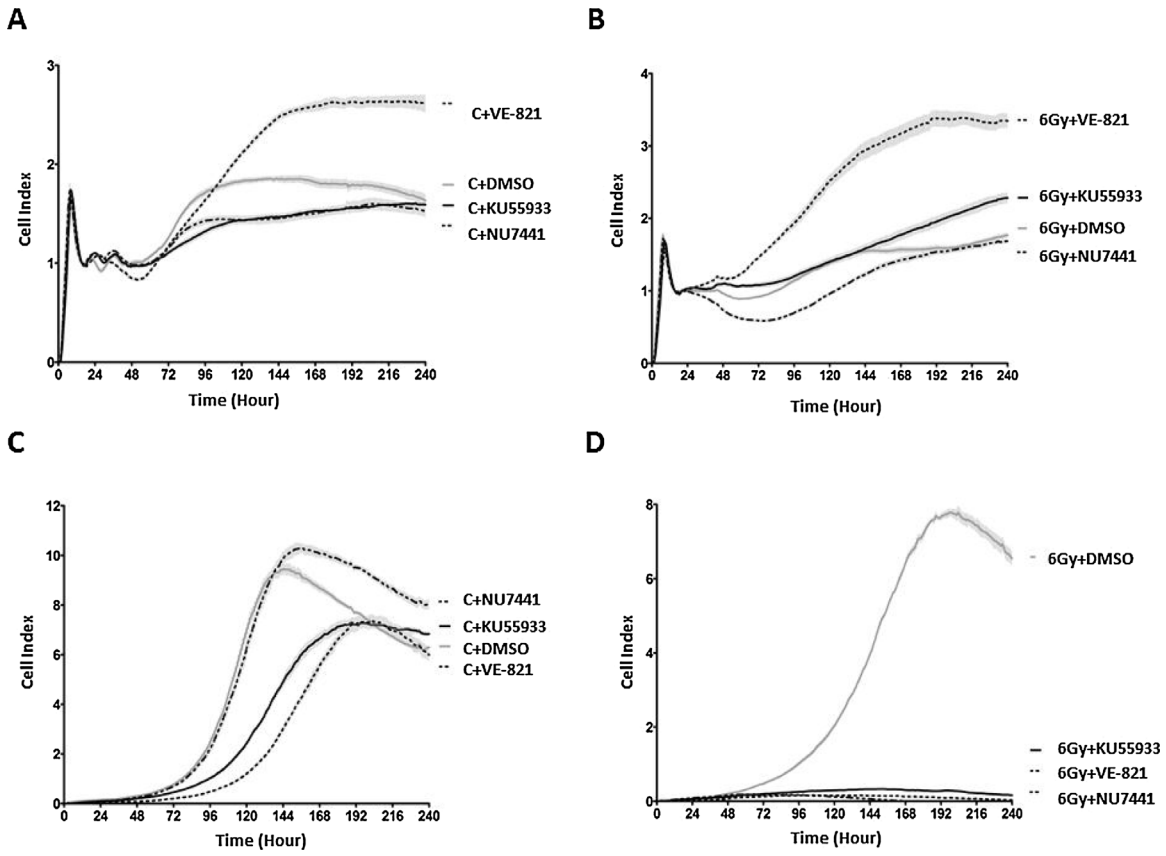

Fig. 1. Cytotoxic assessment of DNA repair inhibitors by xCELLigence system.
NHLF cell proliferation was not suppressed by IR and ATR inhibition. NHLF cells were left untreated (A) or irradiated by 6 Gy (B) and then cultivated either alone or in combination with DNA repair inhibitor (NU7441, KU55933 or VE-821) in the 96-well plate for 10 days. H1299 cells were left untreated (C) or irradiated by 6 Gy (D) and then cultivated either alone or in combination with DNA repair inhibitor (NU7441, KU55933 or VE-821) in the 96-well plate for 10 days. The values represent the mean of six replicates.

detection kit (BM Chemiluminiscence-POD, Roche, Manheim, GER) by exposure to a film.

Statistical analysis

Data presented are means with standard deviation (SD). The data obtained by fluorescence microscopy are presented as median. The data were statistically analysed by *t*-test using SigmaStat software (Aspire Software International, Ashburn, VA, USA). The Mann–Whitney test was used for nonparametric data sets. The differences were considered significant at the significance level $2\alpha = 0.05$.

Results

NHLF cell proliferation was not suppressed by VE-821 and 6Gy

The xCELLigence assay is based on a measurement of changes in electrical impedance which monitor cell proliferation, adhesion, phenotype, and viability (see Material and methods). The impedance values are presented as Cell Index (CI) (Ke et al., 2011). The xCELLigence system was used for cytotoxic effect assessment of the DNA repair inhibitors alone and in combination with IR. For both cell lines, proliferation was measured continuously every hour for 10 days.

For NHLF cells, VE-821 was the least toxic, since after treatment with this the NHLF cells reached an even higher value of CI than the control group after 10 days of continual incubation (Fig. 1A). IR-induced inhibition of NHLF cells proliferation was slightly enhanced by NU7441 pre-treatment (Fig. 1B).

For H1299 cells, treatment with either KU55933 or VE-821 inhibitor resulted in a decrease in H1299 cell proliferation in a similar manner as in the solely irradiated group (Fig. 1C). The combination of IR with any of the applied inhibitors caused an obvious decrease in H1299 cell proliferation in all groups (Fig. 1D).

NU7441 caused the most pronounced and persistent DNA damage in both cell lines after IR

We measured the γH2AX signal in both cell lines 1, 24 and 72 h after IR (Fig. 2A,B). Since we used a 6 Gy dose the foci began to merge. Therefore we had to use integral optical density for the results evaluation.

In NHLF cells, we observed a statistically significant increase in the amount of γH2AX signal compared to the control group 1, 24 and 72 h after irradiation. However, the IR-induced γH2AX signal declined rapidly. IR in combination with NU7441 markedly increased the γH2AX signal 24 h after irradiation, which persisted even 72 h after the treatment. The combination of IR and KU55933 almost abrogated the γH2AX signal in NHLF cells in all studied time intervals. The γH2AX signal caused by IR and VE-821 decreased rapidly in a similar manner to the irradiation-only group.

In H1299 cells, IR induced a pronounced increase in γH2AX signal 1 h after irradiation compared to the control group. However, the DNA damage caused by IR declined rapidly. Similarly to NHLF cells, the DNA damage caused by IR and NU7441 persisted even 72 h after irradiation. The IR and KU55933 combination almost abrogated the γH2AX signal in H1299 cells in all studied time intervals. On the other hand, the γH2AX signal induced by IR and VE-821 combination was higher compared to the IR and NU7441 treated group 1 h after irradiation, but it declined rapidly.

The combination of IR with particular inhibitors affects diverse cell cycle phases

To further determine whether observed DNA damage had an impact on the particular cell cycle phases, the cell cycle was analyzed in both cell lines 24 and 72 h after irradiation.

After NHLF cells were exposed to IR, we observed a moderate increase in G0/G1 phase and a decrease in S phase 24 h after irradiation (Fig. 3A) as well as 72 h after irradiation (Fig. 3B). The combination of IR and NU7441 induced G2/M arrest (31%) in NHLF cells 24 h after irradiation compared to the irradiated group (18%), which was doubled after 72 h after irradiation. The IR and KU55933 treatment resulted in milder G2/M arrest 72 h after irradiation (29%). The combination of IR and VE-821 caused transient increase in G0/G1 phase (89%) compared to the irradiated group (80%) 24 h after irradiation. The effect was no longer observed 72 h after irradiation.

In H1299 cells, IR slightly increased the amount of cells in G0/G1 24 h after irradiation (Fig. 3C). On the other hand, we observed G2/M arrest (30%) in the irradiated group compared to the control (20%) 72 h after irradiation (Fig. 3D). Both NU7441 and KU55933 treatment with IR resulted in G2/M arrest in H1299 cells 24 h after irradiation. Surprisingly, the amount of cells in G2/M arrest decreased to 55% in the IR and NU7441 treated group compared to the IR and KU55933 group, where the G2/M arrest increased (47%) 72 h after irradiation. A slightly higher G2/M arrest (35%) was observed after IR and VE-821 treatment compared to the irradiated group (30%) 72 h after irradiation.

DNA repair inhibitors modulate phosphorylations of DNA damage-signaling proteins

To assess the impact of inhibitors on DNA damage-signaling proteins, alterations of CHK1 and CHK2 proteins were examined by western blotting in both cell lines.

CHK1 and CHK2 proteins play pivotal roles in cell cycle regulation within DDR. The IR exposure increased phosphorylation of CHK1 and CHK2 proteins (Fig. 4A,B). The ATM-mediated phosphorylation of CHK2 T68 was decreased in both cell lines 2 h after irradiation of KU55933-treated cells compared to the irradiated-only group. In contrast, the phosphorylation increased after the IR and VE-821 treatment in both cell lines. The IR-induced phosphorylation of CHK1 S296 2 h after irradiation of VE-821-treated cells was decreased compared to the irradiated-only group in H1299 cells (Fig. 4B). Since we were unable to detect CHK1 S317 or CHK1 S296 phosphorylated forms in NHLF and the CHK1 S317 phosphorylated form in H1299 cells by western blotting, we therefore used ELISA assay to assess CHK1 S317 and CHK2 T68.

By ELISA assay, a minor increase in CHK1 S317 level was measured in H1299 cells after irradiation (Fig. 4C). The CHK1 S317 was more phosphorylated in the IR and KU55933 group compared to the solely-irradiated group in H1299 cells. The up-regulation declined slightly after IR and VE-821 treatment. We did not observe any changes in phosphorylation of CHK1 in NHLF cells.

IR increased the level of CHK2 T68 protein in both cell lines 2 h after irradiation (Fig. 4D). We observed an increase in the level of the protein in IR and NU7441 or VE-821 combinations compared to the solely-irradiated group in H1299 cells. After the IR and KU55933 treatment, a decrease in phosphorylation of CHK2 was observed in both cell lines. These observations corresponded to results obtained by western blotting.

More than one cell death mechanism is triggered in H1299 cells after IR

To assess the impact of inhibitors on proteins involved in cell death in both cell lines, alterations of proteins involved in autophagy (LC3 I and II) and apoptosis (PARP-1) were examined in both cell lines by western blotting 12, 24 and 48 h after irradiation (Fig. 5A,B).

The LC3I/LC3II ratio increased after IR in combination with either KU55933 or VE-821 treatment compared to the irradiated-only group in NHLF cells. The cleavage of LC3 protein was most pronounced in the IR and VE-821 treated group 24 h after irradiation in NHLF cells. Similarly as with NHLF cells, we observed the greatest increase in LC3I/LC3II ratio in the IR and VE-821 treated group 24 and 48 h after irradiation of H1299 cells.

We did not observe any PARP-1 cleavage in NHLF cells. On the other hand, we detected elevated PARP-1 cleavage in H1299 cells 24 and 48 h after IR and NU7441 treatment compared to the group treated solely with IR or in combination with other inhibitors.

Using flow cytometry, we assessed the number of apoptotic cells (Annexin V-positive/PI-negative) in both cell lines.

None of the inhibitors had a statistically significant impact on apoptosis induction in NHLF cells (Fig. 5C).

Any combination of IR and inhibitor led to increased induction of apoptosis compared to the solely-irradiated group in H1299 cells (Fig. 5D). The most pronounced effect was detected after IR and NU7441 treatment (Table 1).

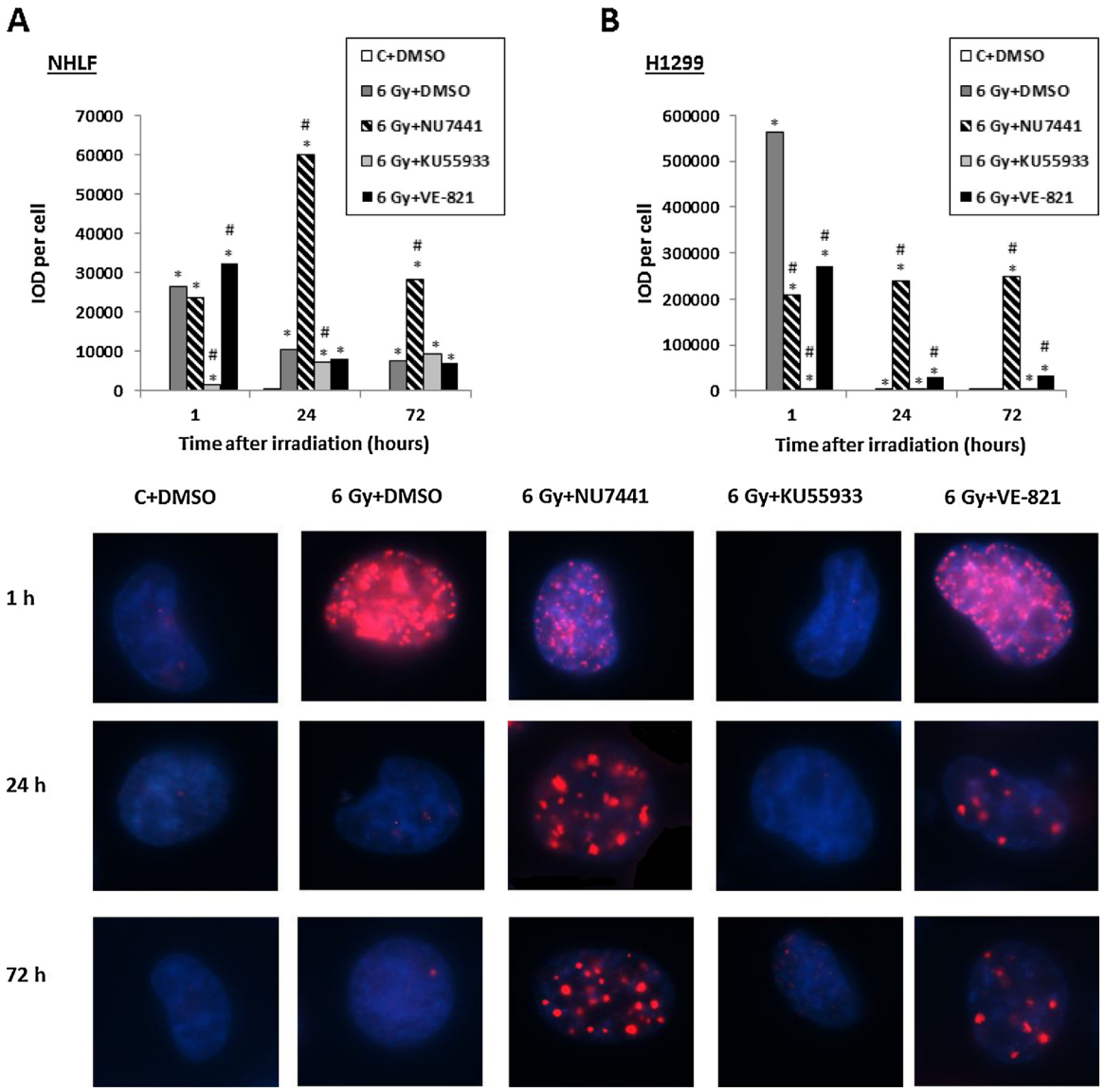

Fig. 2. Accumulation of DNA damage in the form of phosphorylation of histone H2AX.
DNA-PK inhibition induced the greatest DNA damage in both cell lines after IR. NHLF cells (A) and H1299 cells (B) were irradiated by the dose of 6 Gy in the absence or presence of different DNA repair inhibitors (NU7441, KU55933 and VE-821) and the integral optical density of γH2AX (IOD) was determined by immunofluorescence microscopy 1, 24 and 72 h post-irradiation; The results are presented as median of γH2AX IOD per 50 cells. Significant differences ($P < 0.05$) in the γH2AX IOD in comparison to control cells are marked by *, significant differences ($P < 0.05$) in the γH2AX IOD between IR and IR + inhibitor groups are marked by #; (C) representative photographs of γH2AX IOD in NHLF cells; (D) representative photographs of γH2AX IOD in H1299 cells.

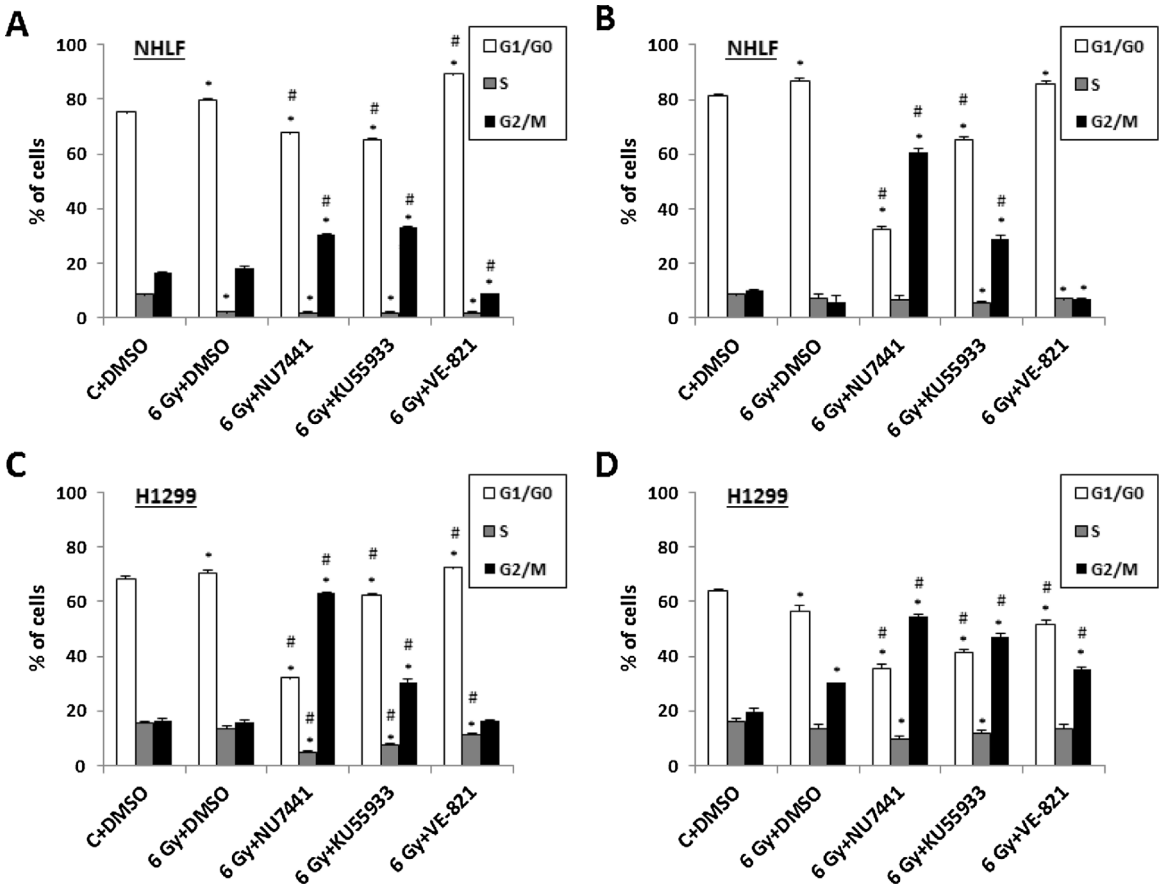

Fig. 3. Impact of DNA repair inhibitors on cell cycle phases.
The DNA repair inhibitors in combination with IR affect different cell cycle phases. NHLF cells were irradiated by 6 Gy in the absence or presence of DNA repair inhibitors (NU7441, KU55933 or VE-821), and the cell cycle was measured 24 h (A) and 72 h (B) after irradiation. H1299 cells were irradiated by 6 Gy in the absence or presence of DNA repair inhibitors (NU7441, KU55933 or VE-821), and the cell cycle was measured 24 h (C) and 72 h (D) after irradiation. Results are the means and SD of three independent experiments. Significant differences ($P < 0.05$) compared to control cells are marked by *, significant differences ($P < 0.05$) between IR and IR + inhibitor groups are marked by #.

Discussion

In this study, we investigated the radio-sensitizing potential of DNA-PK inhibitor NU7441, ATM inhibitor KU55933, and ATR inhibitor VE-821. Since many cancers possess a mutation in the p53 protein, we employed non-small cell lung cancer cells (H1299, p53-deficient). H1299 cells are considered a model relevant to radiotherapy, because non-small cell lung cancer cells are regularly treated by IR. To find out whether the effect of inhibitor is delimited only to the cancer cells, we compared our results with normal human lung fibroblast cells (NHLF, p53-wt). Both cell lines are considered as comparable, but it should be noted that fibroblasts are more resistant to apoptosis and in the case of cell damage they tend to inhibit cell growth by cell cycle arrest and senescence. In contrast to NHLF cells, H1299 cells representing endothelial cells are more predisposed to apoptosis induction after severe cell damage (An et al., 1998; Fuks et al., 1994; Gorbunova et al., 2002).

After exposure to IR, so-called ionizing radiation-induced foci (IRIF) are formed (Giunta et al., 2010). The γH2AX protein is formed at the site of IRIF to promote DNA damage-signalling and subsequent repair. In order to assess DSB repair we employed γH2AX signal measurement. Our results confirmed that phosphorylation of H2AX is mostly ATM-dependent, evidenced by almost completely abrogated DDR after ATM inhibition in combination with IR in both cells. DNA-PK and ATR inhibition in combination with IR had only a partial and transient effect on H2AX phosphorylation, since the γH2AX signal decreased in both cell lines. After the combination of IR and VE-821 we observed a partial decrease in γH2AX signal in comparison with solely-irradiated H1299 cells. We can argue that ATM-mediated phosphorylation of γH2AX is ATR-dependent. For instance, Kmochova et al. (2016) reported that VE-821 caused mild but significant decrease in γH2AX in irradiated human peripheral lymphocytes. Although the exact mechanism remains unclear, we might speculate that H2AX phosphorylation is regulated by ATR via minor lesions activating nucleotide excision repair-dependent and −independent pathways similarly to confluent G_0/G_1 fibroblasts exposed to UV radiation.

The most pronounced effect (delayed DSB repair) was observed in both cell lines after irradiation and DNA-PK inhibition. There is a hypothesis that inhibited DNA-PK kinase activity presumably prevents dissociation of DNA-PK from the DNA ends, and thus blocks two main repair pathways NHEJ and HR (Allen et al., 2003). It has been also reported that due to the failure of DNA-PK to disassociate from the DNA ends, the cells showed a decrease in processing oxidatively-induced non-DSB clustered DNA lesions (Peddi et al., 2010). Both of these theories could explain persistence of the DNA damage caused by IR and NU7441 in both cell lines even 72 h after irradiation.

We focused on signalling pathways and the cell cycle checkpoints which are regulated, in part, by CHK1 and CHK2. After DNA damage, CHK1 is phosphorylated at S317 and S345, which promotes autophosphorylation at S296 (Parsels et al., 2011).

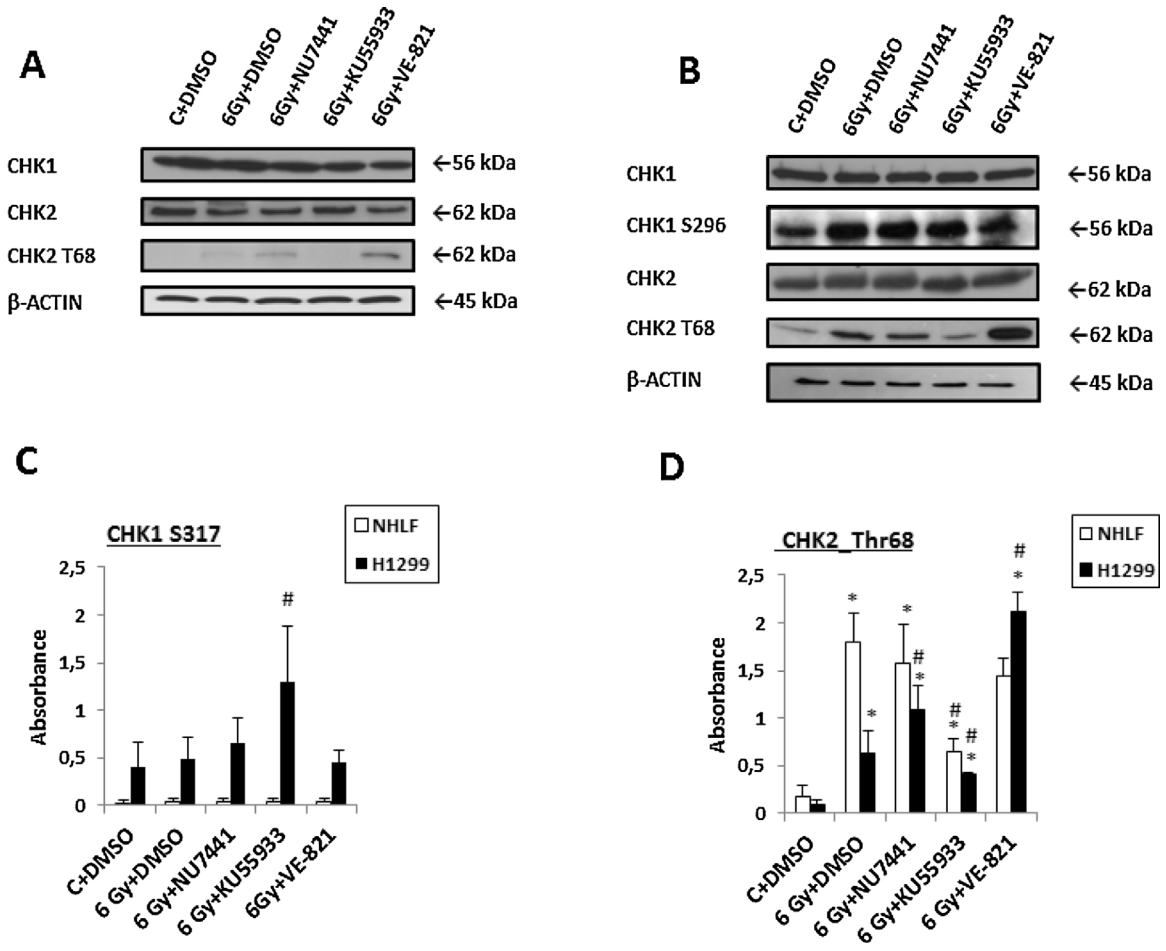

Fig. 4. DNA repair inhibitors modulate phosphorylations of CHK1 and CHK2.
Up-regulation of CHK1 phosphorylated at S317 and CHK2 phosphorylated at T68. DNA repair inhibitors modulate phosphorylations of CHK1 and CHK2 proteins. NHLF cells (A) and H1299 cells (B) were pre-incubated with DNA repair inhibitors (NU7441, KU55933 or VE-821) and exposed to 6 Gy. Whole-cell lysates were analysed 2 h after irradiation. NHLF cells and H1299 cells were pre-incubated with DNA repair inhibitors (NU7441, KU55933 or VE-821) and exposed to 6 Gy. Whole-cell lysates were analysed 2 h post-irradiation. The amount of CHK1 S317 (C) and CHK2 T68 (D) was detected. The values represent the mean of six replicates. Significant differences ($P < 0.05$) compared to control cells are marked by *, significant differences ($P < 0.05$) between IR and IR + inhibitor groups are marked by #.

It was believed that CHK1 phosphorylation is performed by ATR. However, Gatei et al. (2003) showed that this phosphorylation is also executed by ATM. Since we were unable to detect any CHK1 phosphorylation in NHLF cells or CHK1 phosphorylation at S317 in H1299 cells by western blotting (which seems to be a general issue) as, for instance, Gatei et al. (2003), we employed ELISA for assessment of CHK1 S317 phosphorylation. In any case, we did not observe any changes in CHK1 phosphorylation after IR or inhibitor treatment in the NHLF cells. Moreover, the measured absorbance of CHK1 S317 was very low in NHLF cells, which could explain the failure to detect the phosphorylations by western blotting in NHLF cells. Contrary to NHLF cells, we observed decreased CHK1 phosphorylation at S317 following a decrease in CHK1 autophosphorylation at S296 after irradiation and ATR inhibition in H1299 cells.

CHK2 is an ATM downstream target (Chaturvedi et al., 1999; Jazayeri et al., 2006). The protein is activated by phosphorylation at T68 after IR. ATM is the main kinase responsible for this phosphorylation, although ATR participation has also been reported (Wang et al., 2006). We detected decreased phosphorylation of CHK2 at T68 after ATM inhibition treatment in both cell lines. On the contrary, an increase in phosphorylation of CHK2 at T68 was observed in both cell lines after IR and ATR inhibition treatment. Such finding suggests that ATR inhibition could indirectly activate the ATM/CHK2 pathway, which might compensate for a defective ATR/CHK1 pathway in order to induce G2/M arrest. This was proved by higher CHK2 T68 phosphorylation compared to the solely-irradiated group.

DNA repair inhibitors also proved to have an impact on cell cycle distribution. Pronounced G2/M arrest was detected in both cell lines after DNA-PK inhibition. These findings are supported by the study of Zhuang et al. (2011) who assessed that DNA-PK was pivotal for G2 progression, and inhibition of its activity abrogated progression of mitosis and led to further cell accumulation in the G2/M phase. Whereas G2/M arrest increased in NHLF cells, it declined in H1299 cells 72 h after irradiation and DNA-PK inhibition. In the case of H1299 cells, we can speculate that decrease in G2/M arrest 72 h after irradiation and DNA-PK inhibition was caused by i) p53 protein absence supported by the theory of Taylor and Stark (2001) that p53 is essential for maintenance of G2/M arrest; and/or ii) general decrease in the number of the cells because of the induction of apoptosis (indicated by PARP-1 cleavage and flow cytometry data) 48 h after irradiation. This is also consistent with complete proliferation inhibition. The aforementioned findings correspond to the Nikitaki et al. (2015) hypothesis that the targeting of repair protein implicated in more than two entirely distinct DNA repair pathways can lead to synthetic lethality. In our case, this could be inactive DNA-PK and the absence of p53 protein in H1299 cells.

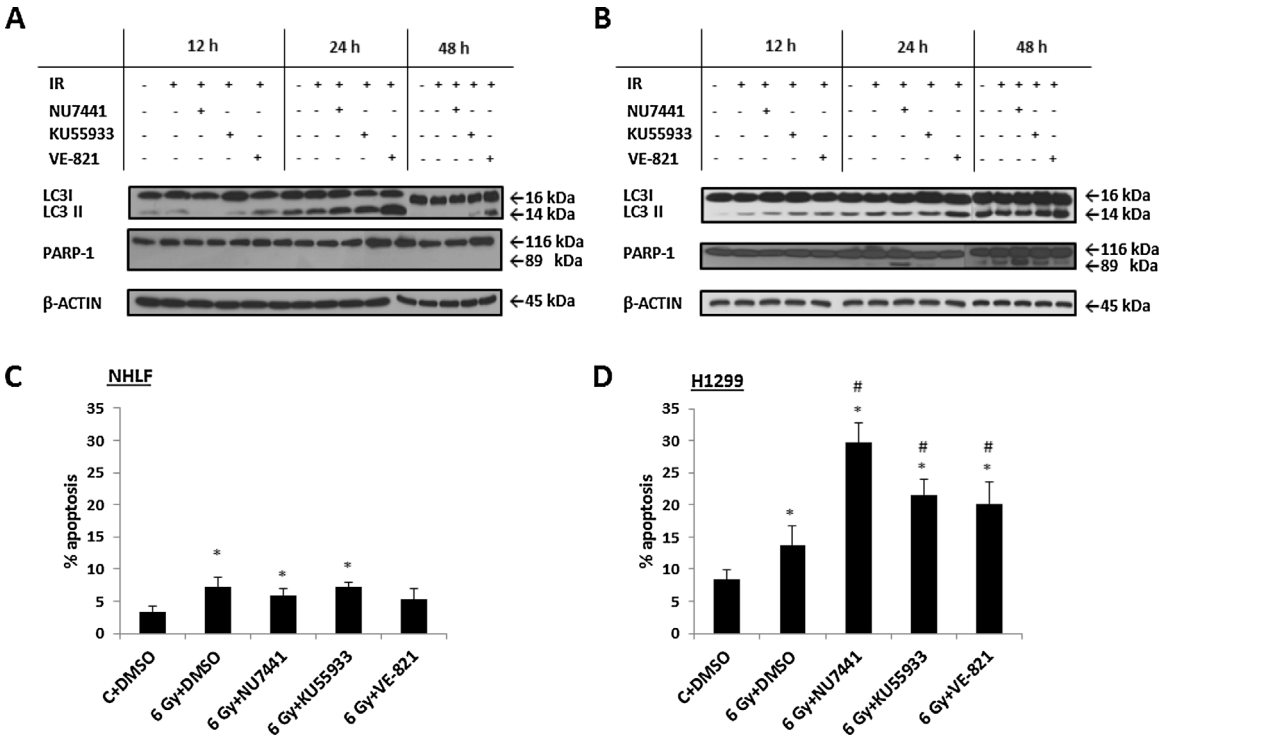

Fig. 5. DNA repair inhibitors induced more than one cell death in H1299 cells.
The highest number of apoptic H1299 cells was found after a combination of IR and NU7441 in H1299 cells. NHLF cells (A) and H1299 cells (B) were irradiated by 6 Gy in the absence or presence of DNA repair inhibitors (NU7441, KU55933 or VE-821). Whole-cell lysates were prepared 12, 24 and 48 h post-irradiation. Autophagy and apoptosis-associated proteins were detected. β-ACTIN was used as a gel loading control. NHLF cells (C) and H1299 cells (D) were pre-incubated with DNA repair inhibitors (NU7441, KU55933 or VE-821) and exposed to 6 Gy. The apoptosis was determined by flow cytometry 48 h after irradiation. Results are the means and SD of three independent experiments. Significant differences ($P < 0.05$) compared to control cells are marked by *, significant differences ($P < 0.05$) between IR and IR + inhibitor groups are marked by #.

As in the case of DNA-PK inhibition, G2/M arrest was detected in both cell lines after irradiation and ATM inhibition. Since NHLF cells are p53-wt we hypothesize that G2/M arrest after irradiation and ATM inhibition was initiated by p53 and presumably regulated by ATR. Such a conclusion is consistent with the work of Tibbetts et al. (1999) who reported that p53 was also a target for ATR in response to IR. On the other hand, H1299 cells are p53-deficient. It has been shown that G2/M arrest can be induced by ATR (p53-independently) under certain conditions (Liu et al., 2012; Taylor and Stark, 2001). Therefore, we suggest that G2/M arrest after irradiation and ATM inhibition was mediated by ATR in both cell lines but via different mechanisms. Comparing G2/M arrest caused by irradiation and DNA-PK and ATM inhibition we can hypothesize that irradiation and DNA-PK inhibition led to greater DNA damage; hence higher G2/M arrest was induced compared to ATM inhibition in both cell lines. After irradiation and DNA-PK inhibition, we also observed higher induction of apoptosis in H1299 cells.

The G2/M phase was relatively stable in NHLF cells, while G2/M arrest was induced in H1299 cells 72 h after irradiation and ATR inhibition. We can hypothesize that higher DNA damage caused in H1299 cells after irradiation and ATR inhibition, was responsible for G2/M arrest induction in H1299 cells compared to NHLF cells. This is evidenced by i) almost complete inhibition of cell proliferation; and ii) PARP-1 cleavage and induction of apoptosis, compared to NHLF cells where no such effect on proliferation, PARP-1 cleavage or apoptosis was observed after irradiation and ATR inhibition. Since we did not observe either a radio-sensitizing effect on NHLF proliferation or a markedly impaired cell cycle compared to the solely-irradiated group in NHLF cells after irradiation and ATR inhibition, we can hypothesize that NHLF cells were able to repair the DNA damage. Our results support the

Table 1
Summary of the results.

	NHLF			H1299		
Parameter	6 Gy + NU7441	6 Gy + KU55933	6 Gy + VE-821	6 Gy + NU7441	6 Gy + KU55933	6 Gy + VE-821
Cell viability	equal	↑	↑	↓	↓	↓
γH2AX signal	↑	equal	equal	↑	equal	↑
Cell cycle	G2 arrest	G2 arrest	equal	G2 arrest	G2 arrest	G2 arrest
CHK1 S317	equal			equal	↑	equal
CHK2 T68	equal	↓	equal	↑	↓	↑
LC3I/II cleavage	equal	↑	↑	equal	equal	↑
PARP-I cleavage	no cleavage observed			↑	equal	↓
Apoptosis	equal	equal	equal	↑	↑	↑

Note: The presented symbols show the differences between the 6 Gy + DMSO group and the other particular groups after irradiation and inhibitor application. ↑ represents statistically significant increase compared to 6 Gy+ DMSO in the parameter; ↓ represents statistically significant decrease compared to 6 Gy + DMSO in the paramater; if equal is noted, there was no statistically significant change compared to the 6 Gy + DMSO group in the parameter.

findings of Pires et al. (2012) who reported a pronounced and cell type-independent radio-sensitizing effect of ATR inhibition (by VE-821 inhibitor) in different kinds of cancer cell lines. Such effect could be caused by a defective ATM-p53 pathway (Reaper et al., 2011).

Conclusion

Taken together, our data showed that DNA-PK, ATM, and ATR kinases play an important role in radiation-induced DDR in normal human lung fibroblasts (NHLF) and non-small cell lung cancer cells (H1299). Phosphorylation of histone H2AX was mainly dependent on ATM presence/function. After either DNA-PK or ATR inhibition, the γH2AX signal was increased due to abrogation of DNA repair mechanisms. ATM was responsible for CHK2 phosphorylation, whereas ATR phosphorylated CHK1 after IR.

In NHLF cells, DNA-PK inhibition (NU7441) combined with IR induced the gravest DNA damage (evidenced by DSB), which persisted 72 h after irradiation. Moreover, NU7441 and ATM inhibition (KU55933) increased G2-arrest. On the other hand, ATR inhibition (VE-821) had a minimal impact on proliferation and cell cycle in NHLF cells.

VE-821 combined with IR caused pronounced inhibition of cell proliferation, induced G2/M-arrest, and triggered apoptosis, and thus diminished DNA-repair of H1299 cells, although not NHLF cells. In conclusion, our results suggest that ATR inhibition could be a promising therapeutic strategy in p53-deficient lung tumours. Importantly, VE-821 displayed minimal cytotoxicity towards the normal cells, which remains a key question of clinical trials aimed to increase the efficacy of radiotherapy. Undoubtedly further work is needed in order to demonstrate the benefits of this approach *in vivo*, but this study contributes to the concept of ATR inhibition and underlines the recent effort to develop novel, highly-selective and non-toxic ATR inhibitors, which are being sought intensively.

Conflict of interests

The authors declare no conflict of interest. The founding sponsors had no role in the design of the study; in the collection, analyses, or interpretation of data; in the writing of the manuscript, and in the decision to publish the results.

Acknowledgments

The authors would like to thank to Ms. Lenka Mervartová for her excellent technical assistance. This work was supported by Ministry of Defence and Ministry of Education and Youth, Czech Republic (project: Long-term organization development plan 1011 and project of specific research: MSMT SV/FVZ201304).

References

Ćmielová, J., Havelek, R., Vávrová, J., Řezáčová, M., 2015. Changes in the response of MCF-7 cells to ionizing radiation after the combination of ATM and DNA-PK inhibition. Med. Oncol. 32, 138.

Allen, C., Halbrook, J., Nickoloff, J.A., 2003. Interactive competition between homologous recombination and non-homologous end joining. Mol. Cancer Res. 1, 913–920.

An, B., Goldfarb, R.H., Siman, R., Dou, Q.P., 1998. Novel dipeptidyl proteasome inhibitors overcome Bcl-2 protective function and selectively accumulate the cyclin-dependent kinase inhibitor p27 and induce apoptosis in transformed but not normal, human fibroblasts. Cell Death Differ. 5, 1062–1075.

Andrs, M., Korabecny, J., Jun, D., Hodny, Z., Bartek, J., Kuca, K., 2015. Phosphatidylinositol 3-Kinase (PI3K) and phosphatidylinositol 3-kinase-related kinase (PIKK) inhibitors: importance of the morpholine ring. J. Med. Chem. 58, 41–71.

Baumann, P., West, S.C., 1998. DNA end-joining catalyzed by human cell-free extracts. PNAS 95, 14066–14070.

Chaturvedi, P., Eng, W.K., Zhu, Y., Mattern, M.R., Mishra, R., Hurle, M.R., et al., 1999. Mammalian Chk2 is a downstream effector of the ATM-dependent DNA damage checkpoint pathway. Oncogene 18, 4047–4054.

Christodoulou, M., Bayman, N., McCloskey, P., Rowbottom, C., Faivre-Finn, C., 2014. New radiotherapy approaches in locally advanced non-small cell lung cancer. Eur. J. Cancer 50, 525–534.

Ciszewski, W.M., Tavecchio, M., Dastych, J., Curtin, N.J., 2014. DNA-PK inhibition by NU7441 sensitizes breast cancer cells to ionizing radiation and doxorubicin. Breast Cancer Res. Treat. 143, 47–55.

Fuks, Z., Persaud, R.S., Alfieri, A., McLoughlin, M., Ehleiter, D., Schwartz, J.L., et al., 1994. Basic fibroblast growth factor protects endothelial cells against radiation-induced programmed cell death *in vitro* and *in vivo*. Cancer Res. 54, 2582–2590.

Gérard, C., Debruyne, C., 2009. Immunotherapy in the landscape of new targeted treatments for non-small cell lung cancer. Mol. Oncol. 3, 409–424.

Gatei, M., Sloper, K., Sorensen, C., Syljuäsen, R., Falck, J., Hobson, K., et al., 2003. Ataxia-telangiectasia-mutated (ATM) and NBS1-dependent phosphorylation of Chk1 on Ser-317 in response to ionizing radiation. J. Biol. Chem. 278, 14806–14811.

Giunta, S., Belotserkovskaya, R., Jackson, S.P., 2010. DNA damage signaling in response to double-strand breaks during mitosis. J. Cell Biol. 190, 197–207.

Gorbunova, V., Seluanov, A., Pereira-Smith, O.M., 2002. Expression of human telomerase (hTERT) does not prevent stress-induced senescence in normal human fibroblasts but protects the cells from stress-induced apoptosis and necrosis. J. Biol. Chem. 277, 38540–38549.

Hirao, A., Kong, Y.Y., Matsuoka, S., Wakeham, A., Ruland, J., Yoshida, H., et al., 2000. DNA damage-induced activation of p53 by the checkpoint kinase Chk2. Science 287, 1824–1827.

Hurley, P.J., Wilsker, D., Bunz, F., 2007. Human cancer cells require ATR for cell cycle progression following exposure to ionizing radiation. Oncogene 26, 2535–2542.

Jazayeri, A., Falck, J., Lukas, C., Bartek, J., Smith, G.C.M., Lukas, J., Jackson, S.P., 2006. ATM- and cell cycle-dependent regulation of ATR in response to DNA double-strand breaks. Nat. Cell Biol. 8, 37–45.

Ke, N., Wang, X., Xu, X., Abassi, Y.A., 2011. The xCELLigence system for real-time and label-free monitoring of cell viability. Methods Mol. Biol. 740, 33–43.

Kmochova, A., Tichy, A., Zarybnicka, L., Sinkorova, Z., Vavrova, J., Rehacek, V., et al., 2016. Modulation of ionizing radiation-induced effects by NU7441, KU55933 and VE821 in peripheral blood lymphocytes. J Appl. Biomed. 14, 19–24.

Lane, D.P., 1992. Cancer. p53 guardian of the genome. Nature 358, 15–16.

Liu, S., Opiyo, S.O., Manthey, K., Glanzer, J.G., Ashley, A.K., Amerin, C., et al., 2012. Distinct roles for DNA-PK: ATM and ATR in RPA phosphorylation and checkpoint activation in response to replication stress. Nucleic Acids Res. 40, 10780–10794.

Nikitaki, Z., Michalopoulos, I., Georgakilas, A.G., 2015. Molecular inhibitors of DNA repair: searching for the ultimate tumor killing weapon. Future Med Chem. 7, 1543–1558.

Parsels, L.A., Qian, Y., Tanska, D.M., Gross, M., Zhao, L., Hassan, M.C., et al., 2011. Assessment of Chk1 phosphorylation as a pharmacodynamic biomarker of Chk1 inhibition. Clin. Cancer Res. 17, 3706–3715.

Peddi, P., Loftin, C.W., Dickey, J.S., Hair, J.M., Burns, K.J., Aziz, K., et al., 2010. DNA-PKcs deficiency leads to persistence of oxidatively induced clustered DNA lesions in human tumor cells. Free Radic. Biol. Med. 48, 1435–1443.

Pires, I.M., Olcina, M.M., Anbalagan, S., Pollard, J.R., Reaper, P.M., Charlton, P.A., et al., 2012. Targeting radiation-resistant hypoxic tumour cells through ATR inhibition. Br. J. Cancer 107, 291–299.

Reaper, P.M., Griffiths, M.R., Long, J.M., Charrier, J.-D., Maccormick, S., Charlton, P.A., et al., 2011. Selective killing of ATM- or p53-deficient cancer cells through inhibition of ATR. Nat. Chem. Biol. 7, 428–430.

Schiller, J.H., Harrington, D., Belani, C.P., Langer, C., Sandler, A., Krook, J., et al., 2002. Comparison of four chemotherapy regimens for advanced non-small-cell lung cancer. New Engl. J. Med. 346, 92–98.

Taylor, W.R., Stark, G.R., 2001. Regulation of the G2/M transition by p53. Oncogene 20, 1803–1815.

Tibbetts, R.S., Brumbaugh, K.M., Williams, J.M., Sarkaria, J.N., Cliby, W.A., Shieh, S.-Y., et al., 1999. A role for ATR in the DNA damage-induced phosphorylation of p53. Genes Dev. 13, 152–157.

Tichy, A., Durisova, K., Salovska, B., Pejchal, J., Zarybnicka, L., Vavrova, J., et al., 2014. Radio-sensitization of human leukaemic MOLT-4 cells by DNA-dependent protein kinase inhibitor, NU7441. Radiat. Environ. Biophys. 53, 83–92.

Toledo, L.I., Altmeyer, M., Rask, M.-B., Lukas, C., Larsen, D.H., Povlsen, L.K., et al., 2013. ATR prohibits replication catastrophe by preventing global exhaustion of RPA. Cell 155, 1088–1103.

Vávrová, J., Zárybnická, L., Lukášová, E., Řezáčová, M., Novotná, E., Sinkorová, Z., et al., 2013. Inhibition of ATR kinase with the selective inhibitor VE-821 results in radiosensitization of cells of promyelocytic leukaemia (HL-60). Radiat. Environ. Biophys. 52, 471–479.

Wang, X.Q., Redpath, J.L., Fan, S.T., Stanbridge, E.J., 2006. ATR dependent activation of Chk2. J. Cell. Physiol. 208, 613–619.

Zhao, H., Watkins, J.L., Piwnica-Worms, H., 2002. Disruption of the checkpoint kinase 1/cell division cycle 25A pathway abrogates ionizing radiation-induced S and G2 checkpoints. PNAS 99, 14795–14800.

Zhuang, L., Cao, Y., Xiong, H., Gao, Q., Cao, Z., Liu, F., et al., 2011. Suppression of DNA-PKcs and Ku80 individually and in combination: Different effects of radiobiology in HeLa cells. Int. J. Oncol. 39, 443–451.